Comparison of spectroscopic properties of Yb:YAP and Yb:YAG crystals

Xiaoming He (何晓明), Guangjun Zhao (赵广军), Xiaodong Xu (徐晓东), Xionghui Zeng (曾雄辉), and Jun Xu (徐 军)

Shanghai Institute of Optics and Fine Mechanics, Chinese Academy of Sciences, Shanghai 201800

Received January 11, 2007

The Yb:YAG and Yb:YAP crystals have been grown by Czochralski method. The absorption spectra and the fluorescence spectra of Yb:YAG and Yb:YAP crystals have been investigated. It is shown that the Yb:YAG crystal has better laser properties and smaller threshold power than Yb:YAP crystal. In addition, the absorption cross-section of the Yb:YAP crystal is 2.16 times of that of the Yb:YAG crystal, so laser diode pumped Yb:YAG lasing can be easily realized. Because YAP single crystal is anisotropic, it is provided with polarization characteristics.

OCIS codes: 160.3380, 160.4760, 160.5690.

Recent development of InGaAs diode laser has stimulated interest in Yb^{3+} doped solid state materials to be used for high efficiency, high power diode-pumped solid state lasers[1]. The trivalent ytterbium ion's simple $[Xe]^4f^{13}$ electronic structure allows for no excited state absorption, upconversion or concentration quenching. The small Stokes shift (about 650 cm^{-1}) between absorption and emission reduces the thermal loading of the material during laser operation.

Among the numerous Yb-doped crystals, Yb:YAG and Yb:YAP have many other attractive characteristics such as high thermal conductivity, excellent physical and chemical properties of the host material. Yb-doped yttrium-aluminum garnets and perovskites have been primarily developed as infrared (IR) laser media[2]. Moreover, they are also used as scintillation materials, which have good scintillation properties of high light output in the ultraviolet (UV) or visible range and a short decay time. Along with IR ($^2F_{5/2} \rightarrow {}^2F_{7/2}$, peaked at 1.03 mm) emission, Yb^{3+} ions embedded into various host lattices show charge transfer (CT) luminescence, which is very interesting[3−5].

In this paper, Yb:YAG and Yb:YAP crystals were grown by the radio frequency (RF) heating Czochralski (CZ) method with an iridium crucible (80 mm in diameter and 50 mm in height). The starting materials were Y_2O_3 (99.999%), Al_2O_3 (99.999%), Yb_2O_3 (99.999%) and the chemical reaction formulas are Yb:YAP: $Al_2O_3 + (1-x)Y_2O_3 + xYb_2O_3 = 2Y_{1-x}Yb_xAlO_3$, $x = 0.1$; Yb:YAG: $5Al_2O_3 + 3(1-x)Y_2O_3 + 3xYb_2O_3 = 2Y_{3(1-x)}Yb_{3x}Al_5O_{12}$, $x = 0.1$, which were mixed in the stoichiometric ratio. The mixture was ground, extruded to form pieces with diameter close to the inner diameter of the crucible at high pressure, then sintered in an aluminum crucible at 1350 °C for 10 h. The charge was then loaded into the iridium crucibles for crystal growth.

The optimal growth conditions were that pulling and rotation rates were 1 mm/h and 10—20 rpm under the nitrogen or argon atmosphere, respectively. The initial growth boundary in solid-melt was convex towards the melt so that the dislocations and impurity were reduced or eliminated. After that, the growth boundary became flat. In order to prevent the crystal from cracking, the crystal was cooled to room temperature slowly after growth.

Samples of Yb:YAG for spectroscopic measurements were cut out of the boules and surfaces perpendicular to the ⟨111⟩ growth axis were polished. Samples of Yb:YAP for spectroscopic measurements were cut out of the boules and surfaces perpendicular to the ⟨100⟩, ⟨010⟩ and ⟨001⟩ axis were polished, respectively. The thickness of the samples was about 0.6 mm. A JASCO V-570 UV/VIS/NIR spectrophotometer was employed for acquisition of the absorption spectra at room temperature. A TRIAX-550 spectrophotometer with InGaAs laser diode (LD) as the pump source (excited at 940 nm) was employed for acquisition of the fluorescence spectra at room temperature.

Light intensity can be taken for $\log(I_0/I)$, with which the absorption coefficient and the absorption cross-section σ_{abs} can be expressed as

$$\alpha = 2.303L^{-1}\log(I_0/I), \tag{1}$$

$$\sigma_{abs} = 2.303(L \cdot N)^{-1}\log(I_0/I), \tag{2}$$

where L is the thickness of the sample, N is the concentration of Yb^{3+} ions. The emission cross-section σ_{em} is given by[6]

$$\sigma_{em}(\lambda) = \sigma_{abs}(\lambda)(Z_l/Z_u)\exp[(E_{zl} - hc/\lambda)/kT], \tag{3}$$

where Z_l, Z_u, k and E_{zl} represent the partition functions for lower and upper levels, Boltzmann's constant, and zero-line energy. E_{zl} is defined to be the energy separation between the lowest component of upper and lower states, respectively. The values of Z_l, Z_u, and E_{zl} have been provided in Ref. [6].

The absorption of Yb^{3+} in Yb:YAG and Yb:YAP crystals occurs only in the wavelength range of 900—1050 nm, and the spectrum is shown in Fig. 1. There are four main absorption bands in Yb:YAG and Yb:YAP crystals, respectively. Four absorption bands centered at 915, 941, 969, 1029 nm in Yb:YAG crystal were observed and

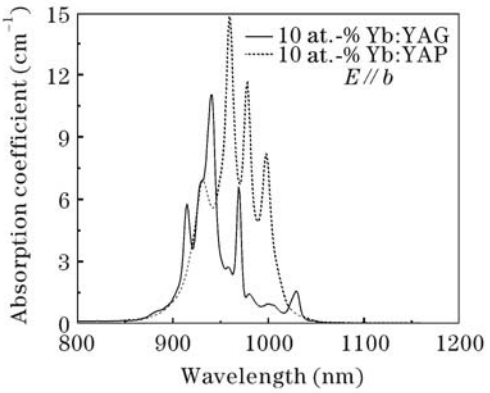

Fig. 1. Absorption spectra of Yb:YAG and Yb:YAP crystals at room temperature.

attributed to the ${}^2F_{7/2} \rightarrow {}^2F_{5/2}$ transition of Yb^{3+} in YAG. Four absorption peaks at 932, 960, 978, 998 nm in Yb:YAP crystal were attributed to the ${}^2F_{7/2} \rightarrow {}^2F_{5/2}$ transition of Yb^{3+} in YAP. In the Yb:YAG crystal, the strongest absorption peak occurs in 941 nm, and the corresponding absorption coefficient is 11.0 cm^{-1}; the absorption full-width at half-maximum (FWHM) is about 20 nm and the absorption cross-section is 0.74×10^{-20} cm^2 as calculated from Eq. (2). In the Yb:YAP crystal, the strongest absorption peak occurs in 960 nm, and the corresponding absorption coefficient is 14.79 cm^{-1}; the absorption linewidth (FWHM) is about 17 nm and the absorption cross-section is 1.51×10^{-20} cm^2 as calculated from Eq. (2). They all have the wide FWHM and large absorption cross-section. A wide FWHM means that laser crystal can accommodate some thermal shift of the pump light wavelength, and the output power of the laser remains stable. Therefore, the FWHM of absorption band at pump wavelength is one of the important parameters for laser crystal. The absorption cross-section of Yb:YAP is 2.16 times of that of Yb:YAG. A large absorption cross-section means that laser crystal is easy to realize LD pumping.

We used the same sample to measure the fluorescence spectra at room temperature, which are shown in Fig. 2. In the spectra, there are several strong broad fluorescence bands in the wavelength range of 950—1150 nm. We can see that four peaks appear at the wavelengths of 969, 1007, 1031, 1048 nm in Yb:YAG and 980, 1000, 1013, 1040 nm in Yb:YAP. They are attributed to the

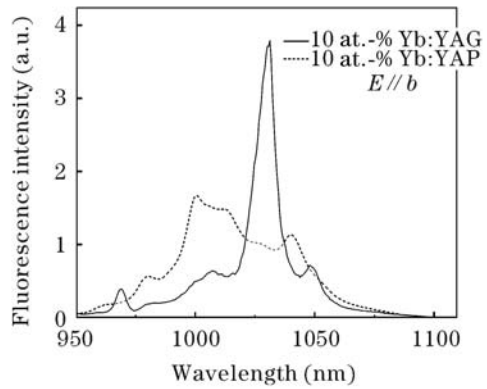

Fig. 2. Fluorescence spectra of Yb:YAG and Yb:YAP crystals at room temperature.

transitions between the lowest energy-level of excited state ${}^2F_{5/2}$ and the ground state ${}^2F_{7/2}$. In the Yb:YAG crystal, the peak at about 1031 nm is the strongest fluorescence peak and the corresponding emission cross-section is 1.86×10^{-20} cm^2 as calculated from Eq. (3). In the Yb:YAP crystal, the peak at about 1000 nm is the strongest, but where the absorption coefficient is very large. So this wavelength cannot be used for practical laser output. The peak at 1013 nm is lower than that at 1000 nm. The absorption coefficient at 1013 nm is very little, so it is a useful wavelength for laser output. And σ_{em} at 1013 nm is 1.20×10^{-20} cm^2 as calculated from Eq. (3).

We can estimate the laser function parameters through the absorption cross-section, the emission cross-section and fluorescence lifetime, such as the emission saturation flounce F_{ext} at the extraction wavelength λ_{ext}, the pump saturation intensity parameter I_{sat}, the minimum pump intensity I_{min}, and the minimum fraction β_{min}.

The emission saturation fluence F_{ext} is given by

$$F_{ext} = hc/(\sigma_{ext}\lambda_{ext}),$$

where σ_{ext} is the value of the emission cross-section (σ_{em}) at the chosen extraction wavelength. Smaller values of F_{ext} allow for simpler means of extraction for the case of a laser amplifier, and also lead to a lower threshold and a continuous wave (CW) oscillator configuration. The actual magnitude of σ_{ext} which is most useful will depend on the pulse length, pumping conditions, damage threshold of the optical components and other factors. For nanosecond range, $\sigma_{ext} > 10^{-20}$ cm^2 is generally required.

The pump saturation intensity parameter I_{sat} is given by

$$I_{sat} = h\nu/(\sigma_{abs}\tau_{em}).$$

For all configurations of efficient diode-pumped Yb-laser systems, it will be necessary to drive a substantial fraction of the ground state Yb ions to the excited state, in order to achieve adequate gain (and to overwhelm the ground state absorption losses). The ease with which this ground state depletion may be accomplished depends on the absorption cross-section σ_{abs} and the emission lifetime τ_{em}. This is described by the pump saturation intensity parameter.

The importance of I_{sat} can be recognized by noting that the fraction of excited Yb ions is given by I_{abs}/I_{sat} in the low doping limit, where I_{abs} is the absorbed pump power. Since InGaAs diode sources are regarded as peak-power-limited devices, clearly a long emission lifetime is favorable in order to accumulate a greater population inversion for a given peak power. We can also calculate the minimum fraction of Yb^{3+} ions that must be excited such that the ground state absorption and the gain exactly balance, and there is net transparency at λ_{ext}.

The minimum fraction β_{min} at the extraction wavelength is given by

$$\beta_{min} = \sigma_{abs}(\lambda_{ext})/[\sigma_{abs}(\lambda_{ext}) + \sigma_{em}(\lambda_{ext})].$$

The minimum pump intensity required to achieve transparency at the extraction wavelength is given by

$$I_{min} = \beta_{min} I_{sat},$$

Table 1. Spectroscopic Parameters of Yb:YAG and Yb:YAP Crystals

Parameter	Yb:YAG	Yb:YAP
λ_{abs} (nm)	941	960
$\Delta\lambda_{abs}$ (nm)	19	17
σ_{abs} ($\times 10^{-20}$ cm^2)	0.8	1.51
λ_{ext} (nm)	1031	1013
σ_{em} ($\times 10^{-20}$ cm^2)	1.86	1.20
τ_{em} (ms)	1.08	0.72
F_{ext} ($\times 10^{23}$ cm^{-3})	10.4	16.4
β_{min}	0.055	0.146
I_{sat} (kW/cm^2)	24	18
I_{min} (kW/cm^2)	1.32	2.63

where we have obtained the I_{min} by setting the fraction of excited Yb ions (I_{abs}/I_{sat}) equal to the required fraction β_{min}, such that $I_{min} = I_{abs}$, I_{min} may be interpreted as the absorbed pump intensity required to reach threshold in an otherwise lossless oscillator, or the absorption and gain become exactly equal at the chosen extraction wavelength λ_{ext} in an amplifier configuration.

In order to make further evaluation on laser properties of Yb:YAG and Yb:YAP, we compared the spectral parameters of the crystal which have been estimated, as listed in Table 1. From the table, we can see that the Yb:YAG crystal has the longest radiative lifetime, which provides good energy storage properties. The F_{ext}, β_{min} and I_{min} of the Yb:YAG crystal are less than that of Yb:YAP crystal, so Yb:YAG has the lower threshold power than Yb:YAP crystal.

Yttrium orthoaluminate, $YAlO_3$, is known to have a perovskite type structure (unit cell parameters: $a = 0.5176$ nm, $b = 0.7355$ nm, $c = 0.5307$ nm, space group: D_{2h}^{16}-Pnma)[7]. Because YAP single crystal is anisotropic, the gain of the medium, polarization characteristics and laser wavelength vary with the orientation of the crystal. The absorption and fluorescence spectra of the crystal with the orientation perpendicular to the b axis have an obvious discrepancy with other axis.

The absorption spectra of different axis Yb:YAP crystal at room temperature are shown in Fig. 3. The absorption peak of b-axis crystal is at 960 nm with absorption coefficient of 14.79 cm^{-1}, while the peaks of a-axis and c-axis crystals are both at 978 nm with absorption

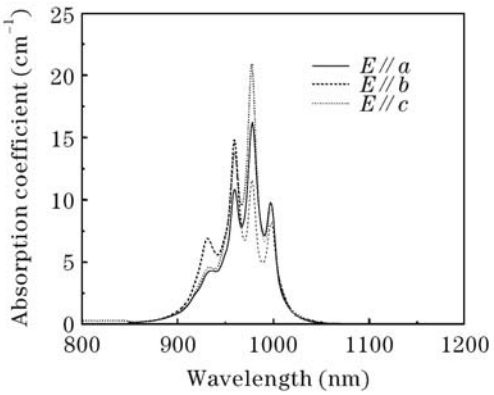

Fig. 3. Absorption spectra of 10 at.-% Yb:YAP at room temperature.

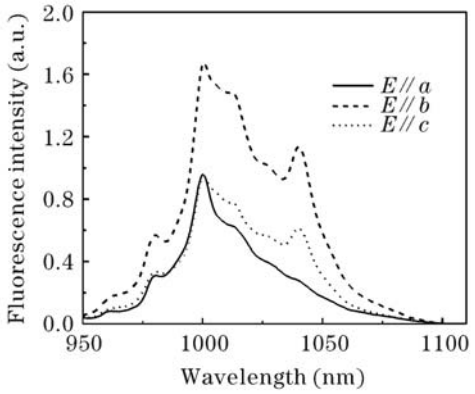

Fig. 4. Fluorescence spectra of 10 at.-% Yb:YAP crystal at room temperature.

coefficients of 16.39 and 20.88 cm^{-1}, respectively. The absorption intensities of a-axis and c-axis crystals are larger than b-axis crystal. The fluorescence spectra of a-, b- and c-axis crystals are shown in Fig. 4, whose peaks are all at 1000 nm. It is interesting that the fluorescence intensity of b-axis crystal is about two times of a- or c-axis crystal. From the absorption and fluorescence spectra, it can be seen that both bands have overlapped. So the self-absorption phenomenon is serious in YAP crystal. Compared with a- and c-axis crystals, the absorption peak of b-axis crystal at 960 nm is more far from the fluorescence band so that the overlap of both bands is little which can reduce the self-absorption phenomenon. The b-axis crystal was the best direction for laser.

In conclusion, the spectroscopic properties of Yb:YAP and Yb:YAG crystals have been compared. The laser function parameters have also been estimated. Our results show that Yb:YAG crystal has better laser properties and little threshold power than Yb:YAP crystal. On the other hand, the absorption cross-section of Yb:YAP is 2.16 times of that of Yb:YAG, LD pump can be easily realized. Because YAP single crystal is anisotropic, it is provided with polarization characteristics. In the Yb:YAP crystal, self-absorption phenomenon is serious. Because the self-absorption of b-axis crystal is less serious than that of other axes, it is the best direction for laser.

X. He's e-mail address is hexiaoming@siom.ac.cn.

References

1. P. Lacovara, H. K. Choi, C. A. Wang, R. L. Aggarwal, and T. Y. Fan, Opt. Lett. **16,** 1089 (1991).
2. W. F. Krupke, IEEE J. Sel. Top. Quantum Electron. **6,** 1287 (2000).
3. L. van Pieterson, M. Heeroma, E. de Heer, and A. Meijerink, J. Lumin. **91,** 177 (2000).
4. I. A. Kamenskikh, N. Guerassimova, C. Dujardin, N. Garnier, G. Ledoux, C. Pedrini, M. Kirm, A. Petrosyan, and D. Spassky, Opt. Mater. **24,** 267 (2003).
5. N. Guerassimova, C. Dujardin, N. Garnier, C. Pédrini, A. G. Petrosyan, I. A. Kamenskikh, V. V. Mikhailin, I. N. Shpinkov, D. A. Spassky, K. L. Ovanesyan, G. O. Shirinyan, R. Chipaux, M. Cribier, J. Mallet, and J.-P. Meyer, Nucl. Instr. and Meth. A **486,** 278 (2002).
6. L. D. Deloach, S. A. Payne, L. L. Chase, L. K. Smith, and W. L. Kway, IEEE J. Quantum Electron. **29,** 1179 (1993).
7. M. J. Weber, M. Bass, K. Andringa, R. R. Monchamp, and E. Comperchio, Appl. Phys. Lett. **15,** 342 (1996).